

A low-power GNSS payload board for precise orbit determination onboard the ARIS SAGE microgravity nanosatellite

Project within the scope of the MSc Geomatics,
Spring Semester 2023

Student Paper

Author(s):

Wicki, Juliette

Publication date:

2023-06

Permanent link:

<https://doi.org/10.3929/ethz-b-000617764>

Rights / license:

[In Copyright - Non-Commercial Use Permitted](#)

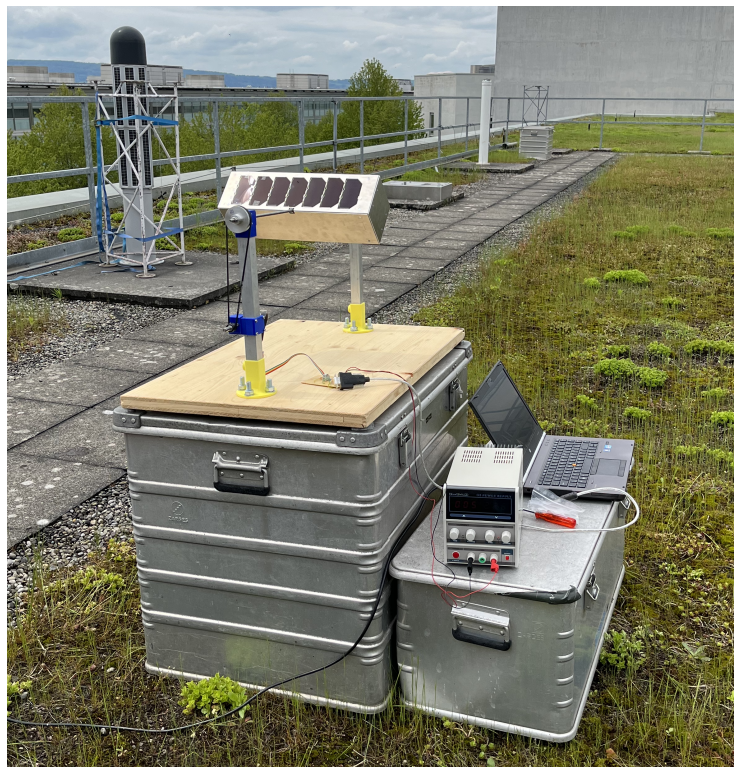


ETH

Eidgenössische Technische Hochschule Zürich
Swiss Federal Institute of Technology Zurich

A low-power GNSS payload board for precise orbit determination onboard the ARIS SAGE microgravity nanosatellite

Project within the scope of the MSc Geomatics, Spring Semester 2023



Juliette Wicki

Supervisors: Prof. Dr. Benedikt Soja, Dr. Gregor Moeller, Alexander Wolf, Julian Moosmann

Chair of Space Geodesy, ETH Zurich

June 2023

Abstract

The mission SAGE by Akademische Raumfahrt Initiative Schweiz (ARIS) examines the aging of human cells in milligravity conditions. Therefore, a low-power GNSS payload board for positioning, precise orbit determination and attitude determination is foreseen to complement the satellite's equipment. This paper defines fundamental technical specifications such as the necessary configurations of the GNSS receivers and describes the implementation to read and parse the received messages. Furthermore, it presents an experiment to analyse the noise behaviour of the received signals.

Contents

1	Introduction	1
2	Methodology	3
2.1	Hardware Components	3
2.1.1	Antennas	3
2.1.2	Receivers	3
2.1.3	Other Components	4
2.2	Software Components	4
2.2.1	Serial Connection	5
2.2.2	Reading and Parsing	5
2.3	Observation Scenarios	5
2.3.1	Nominal PVT Scenario	5
2.3.2	Precise Orbit Determination Scenario	5
2.3.3	Attitude Determination Scenario	6
2.4	Attitude Determination Experiment	6
2.4.1	Study Design	6
2.4.2	Hypotheses	6
2.4.3	Prototype	7
2.4.4	Study Setup and Procedure	7
2.4.5	Data Analysis	7
3	Data	9
3.1	GNSS data	9
3.2	Collected Data	9
3.3	Broadcast Ephemerides	9
4	Results	11
5	Discussion	14
6	Conclusion and Outlook	16
A	Some Additional Results	i

List of Figures

1	Sketch of the CubeSat and the possible antenna mounting spots (green) including the dimensions of the according baselines (not true to scale)	3
2	The experiment setup including the prototype, the mount and the engine	8
3	The prototype with solar panels and three antennas	8
4	Number of tracked satellites during the experiment without solar panels	11
5	Number of tracked satellites during the experiment with solar panels	11
6	The standard deviation of the SNR for all antennas and measurement epochs computed using error propagation (see Formula 1)	12
7	The SNR of the satellite G23 during the experiment without solar panels	12
8	The SNR of the satellite G23 during the experiment with solar panels	12
A.1	For each antenna and measurement epoch the mean of the number of tracked satellites is displayed	i
A.2	Sky-plot of ANT1 during the experiment without solar panels, generated using <i>RTKLIB</i>	i
A.3	SNR of L1, multipath and elevation of satellites tracked by ANT1 during the experiment without solar panels, generated using <i>RTKLIB</i>	ii
A.4	Satellites tracked by ANT1 during the experiment without solar panels, generated using <i>RTKLIB</i> , color-coding represents number of tracked frequencies (green: 2 frequencies, yellow: 1 frequency)	ii
A.5	SNR of L1 of the satellites tracked by ANT1 with the three highest and smallest standard deviations during the experiment without solar panels	iii

List of Tables

1	Communication port configurations	4
2	Abbreviation and explanation (u-blox AG, 2022a) of the enabled GNSS messages as well as the scenario they are used for	6

Acronyms

ADCS	Attitude Determination and Control System. 1, 16
ANT1	Antenna 1. i–iii, 3, 14, III
ANT2	Antenna 2. 3, 9, 14
ANT3	Antenna 3. 3, 9, 14
ARIS	Akademische Raumfahrt Initiative Schweiz. 1, 17, I
ASCII	American Standard Code for Information Interchange. 4
C/N0	carrier noise density. 7
CDDIS	Crustal Dynamics Data Information System. 9
COM	Communication System. 1
CSV	comma-separated values. 5
ECEF	earth centred and earth fixed. 6
EPS	Electrical Power System. 1
GLONASS	Globalnaja nawigazionnaja sputnikowaja sistema. 9
GNSS	Global Navigation Satellite System. 1–7, 9, 14, 16, I, III
GPS	Global Positioning System. 5, 6, 9, 11
NASA	National Aeronautics and Space Administration. 9
OBC	On-Board Computer. 1, 4, 5, 16
PAY	Biological Payload. 1
PCB	printed circuit board. 3
POD	precise orbit determination. 1, 5, 6, I
PVT	position, velocity and timing. 5, 6
RINEX	Receiver Independent Exchange Format. 7, 9
SAGE	Swiss Artificial Gravity Experiment. 1, 3–5, 9, 16
SNR	signal-to-noise ratio. ii, iii, 7, 8, 11–16, III
STR	Structure. 1, 3
TCS	Thermal Control System. 1

1 Introduction

ARIS (Akademische Raumfahrt Initiative Schweiz) is an association with the aim to engage students in different engineering projects related to space exploration. It promotes the collaboration of several Swiss education institutes, such as ETH Zurich, and industry partners. (ARIS, 2023b)

One of their projects, the mission called Swiss Artificial Gravity Experiment (SAGE), focuses on developing and launching a CubeSat in 2025. A CubeSat with its basic unit of 10 times 10 times 10 cm belongs to the class of nanosatellites and serves as a low-cost alternative for larger spacecrafts (Toorian et al., 2008). ARIS' CubeSat consists of three such basic units to investigate the artificial micro- and milligravity generation. These gravity conditions are normally found on small moons and asteroids. The SAGE CubeSat is a first-of-its-kind implementation because it proposes to use a satellite platform as a centrifuge to acquire the desired gravity range. Furthermore, the mission allows to explore the aging of human cells in space. (ARIS, 2023a)

The satellite is launched to a low Earth orbit at altitudes between 300 to 800 km. Therefore, it needs around 1.5 hours to travel around the Earth once. Following a special kind of polar orbit, namely a sun synchronous orbit, it passes roughly over the poles. Sun synchronous orbits are determined to have always the same position relative to the sun. As a result, satellites in a sun synchronous orbit pass the same location on Earth at the same local time. Besides the advantage of observing one location constantly at the same time, sun synchronous orbits can be synchronised so that the satellite moves along the day and night boundary. By permanently riding at dawn and dusk, the satellite is never in the Earth's shadow and can harvest energy continuously using solar panels. (The European Space Agency, 2020)

Seven different subsystems of the satellite ensure the success of the mission (ARIS, 2023a):

- The Structure (STR) of the CubeSat must withstand the different conditions during the launch and in space as well as provide mounting possibilities for the other subsystems.
- The Biological Payload (PAY) is used to investigate the aging of human cells by hosting the first cell culture in space.
- The Thermal Control System (TCS) ensures the operating of the satellite in space by maintaining its temperature within the operating limits.
- The Electrical Power System (EPS) guarantees the generation, storage and provision of power for other subsystems using solar panels, a battery pack and a power distribution module.
- The Communication System (COM) enables to receive data from the satellite, send commands to the satellite and monitor the satellite's health.
- The Attitude Determination and Control System (ADCS) assesses, monitors and adjusts the attitude of the CubeSat by using various sensors, actuators and a state estimation software. Furthermore, it allows the generation of the artificial micro- and milligravity by rotating the satellite up to 1 radian per second.
- The On-Board Computer (OBC) manages as well as processes various tasks of the other subsystems to guarantee the satellite's health. It provides a local data-storage for the experimental data and log information.

To foster the ADCS, a low-power Global Navigation Satellite System (GNSS) payload is included onboard the satellite. It provides equipment to receive and process GNSS data for positioning, precise orbit determination (POD) and attitude determination. This paper focuses on the design and implementation of the GNSS payload. Therefore, the fundamental technical specifications for the integration on board the SAGE CubeSat are defined and a parsing algorithm for the GNSS messages is scripted. Furthermore, various configurations are analysed by conducting an experiment with a rotating prototype.

The section 2.1 describes the hardware components used for the GNSS payload in detail, whereas the section 2.2 focuses on the software implemented. The possible observations using the GNSS payload are listed in section 2.3. Section 2.4 describes the experiment performed on Earth to analyse the received signals while the satellite rotates around itself. The observed data is presented in section 3. The obtained results are listed and discussed in section 4 and 5 respectively. The last section (section 6) focuses on concluding the paper and presenting an outlook for future investigations.

2 Methodology

To equip the CubeSat for the SAGE mission with a GNSS payload, different hardware and software are necessary. Hereafter, various components to enable a successful mission are described. Furthermore, the experiment performed on Earth to validate the received data while the satellite rotates around itself is presented.

2.1 Hardware Components

In general, the following hardware components are needed to receive GNSS data: an antenna, a receiver and cables to connect these two to a processing component. Furthermore, band-pass filters, low-noise amplifiers and splitters can be integrated to improve the quality of the received signals.

2.1.1 Antennas

To enable the attitude determination using a baseline, two low-cost, passive GNSS antennas are deployed, namely the model *GPSF.36.7.A.30* by Taoglas (Taoglas, 2021). For the determination of the orientation in all three directions, a third antenna would be required. However, it is not possible to install three antennas due to limitations within the SAGE mission. The two antennas in use are mounted on a printed circuit board (PCB) on the outside of the satellite to receive the GNSS signal. The baseline between both antennas should be as large as possible. Nevertheless, both antennas should have a common view angle so that identical satellites can be observed for attitude determination. Therefore, the mounting spots represented in Figure 1 are proposed. Either the configuration including Antenna 1 (ANT1) and Antenna 2 (ANT2) or the configuration including Antenna 1 (ANT1) and Antenna 3 (ANT3) should be applied. Otherwise, the baseline is too short. In consultation with the STR team and other subsystems, the configuration including ANT1 and ANT3 is chosen for the CubeSat due to lack of space. The exact mounting spot and therefore the length of the baseline is still in development. The dimensions of the baselines in Figure 1 are the ones used for the prototype of the satellite (see section 2.4).

2.1.2 Receivers

For the SAGE mission, two *ZED-F9P* receivers by u-blox are used (u-blox AG, 2023). They allow to track multiple GNSS constellations (see section 3), which can be selected using the software *u-center* (u-blox AG, 2022b). Among others, this software enables to configure the receivers depending on the tasks (see section 2.3). These individual settings are complemented with general

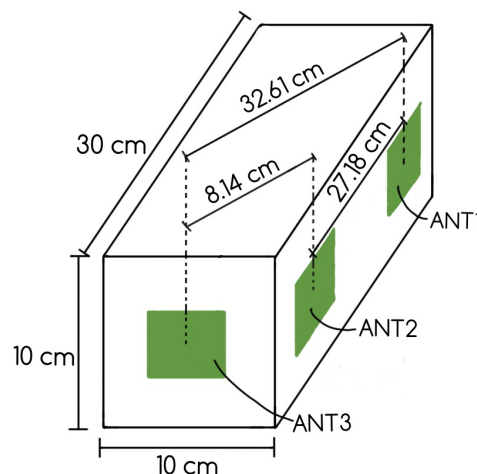


Figure 1: Sketch of the CubeSat and the possible antenna mounting spots (green) including the dimensions of the according baselines (not true to scale)

configurations for the communication port. *ZED-F9P* receivers can communicate via different interfaces, including SPI, I2C, UART and USB (u-blox AG, 2023). The latter two are used for the SAGE mission together with the communication port configurations listed in Table 1. The baud rate is set to the highest possible value and may need to be reduced in the future depending on the driver implemented on the OBC.

Configuration	Value
baud rate	921'600
byte size	8
parity	none
stop bits	1

Table 1: Communication port configurations

To reuse the configurations on other receivers, they are saved to ASCII-files (see supplementary material, in section "4_additional material"). The hexadecimal records in the ASCII-files can easily be loaded on other receivers with the software *u-center* (u-blox AG, 2022b). These configuration files only work on *ZED-F9P* receivers with the same firmware as the one used for setting up the file. For the project, a *ZED-F9P* receiver with firmware version 1.12 was used. For each of the different tasks (see section 2.3), a separate ASCII-file is generated.

2.1.3 Other Components

The antennas on the outside of the satellite are connected via isolated cables to the OBC. The isolation helps to prevent interference with other electronic devices within the satellite that disturb the signal. On the OBC, the receivers as well as band-pass filters, low noise amplifiers and splitters are placed. Band-pass filters allow to only record signals of interest within a certain frequency range. For the SAGE mission, the model *Walsin RBBPF3225180C67B1U* is suggested (Mouser Electronics Inc., 2023). The low noise amplifiers enable analysing the weak signal by amplifying it. Either the models *infineon BGB741L7ESD* (Infineon Technologies AG, 2021) or *Qorvo TQP3M9036* (Qorvo Inc., 2023) are recommended for the SAGE mission. As the CubeSat is planned with the same amount of antennas and receivers, splitters are not necessary. Nevertheless, they increase the redundancy by enabling to connect both antennas to both receivers individually. In case of malfunctioning of one antenna or receiver, it is possible to switch to the other antenna or receiver using the splitters. As a trade-off, the payload software of the OBC gets slightly more complicated because it has to be able to activate the corresponding transistors so that the antenna and receiver in use are supplied with power. The setup of the payload software running on the OBC is not part of the present project. It is suggested to use either the model *Mini-Circuits QCN-19D+* (Mini-Circuits, n.d.[b]) or *Mini-Circuits GP2S1+* (Mini-Circuits, n.d.[a]) for the SAGE mission.

Furthermore, it is essential that all collected GNSS data are available for post-processing on the ground. Therefore, the memory capacity of the OBC must be large enough to store the gathered GNSS observation data until they are downloaded to the ground station. For details about the message size of the GNSS data, the documentation of the observation scenarios in the supplementary material, section "4_additional material" can be consulted. To download the stored observation data, the download data rate must be sufficient. The SAGE mission uses an S-Band link for communication which meets these conditions (ARIS, 2023a).

2.2 Software Components

The following sections aim to give a brief overview of the functionality of the python scripts written for the parsing of the received data. In general, the scripts enable to establish a serial connection to a receiver, read the incoming data and parse it. For a detailed description, consult the readme-file

as well as the commented code in the supplementary material, section "3_code". In addition, the code is shared with the supervisors via gitlab.

The scripts form a basis for the implementation of the payload software running on the OBC.

2.2.1 Serial Connection

If the receiver is connected to a device running the scripts, such as a computer, the serial connection has to be established first. Therefore, the settings in Table 1 are saved in the script *const.py*. The script *generate_config.py* can then be used to set up a file storing these settings. Based on this file, the serial connection is established using the script *read_receiver.py*.

2.2.2 Reading and Parsing

After having established the serial connection, the script *read_receiver.py* can moreover be used to read out the received bytestream. The gathered data is stored in a txt- or ubx-file. The script *txt_ubx2csv.py* allows to parse the recorded data from such files. While parsing, the relevant GNSS messages according to the observation scenarios (see Table 2) can be extracted. The parsed data are saved in a CSV-file designed according to specifications by the supervisors (see section 4).

Furthermore, there is a script, *ser_ubx2csv.py*, that combines the functionalities of two scripts *txt_ubx2csv.py* and *read_receiver.py* by reading and parsing the data directly from the serial connection. This script allows to compare the performance of using an intermediate step to generate a txt-file or directly parsing the data. Evaluations have shown that the intermediate step makes not much of a difference. Nevertheless, the script cannot be used if the receiver is not connected to the device as for example in the experiment described in some of the subsequent subsections.

2.3 Observation Scenarios

To support the SAGE mission, three different observation scenarios are planned for the mission lifetime. The scientific operation of the GNSS payload qualifies as "fully successful" if all the scenarios are carried out according to the specifications. The following subsections describe the scenarios briefly. For further information on the scenarios such as the runtime, the power consumption or the data volume, the detailed documentation in the supplementary material, section "4_additional material" should be considered.

For each of the scenarios, a separate configuration file for the receivers is generated using the software *u-center* (u-blox AG, 2022b) (see section 2.1).

2.3.1 Nominal PVT Scenario

This scenario is the default scenario for the setting of the GNSS receivers during normal operations. Its mission-critical functionality should not be compromised by any of the other scenarios. It provides the position, velocity and timing (PVT) of the satellite with a sampling rate of 10 seconds. Therefore, it uses the PVT data, namely the messages UBX-NAV-PVT, UBX-NAV-POSECEF, UBX-NAV-VELECEF and UBX-NAV-TIMEGPS. Table 2 explains the purpose of each message. For more information about the message protocols see section 3.1.

This scenario requires only one GNSS antenna and one receiver and uses the observations of the four major GNSS constellations, GPS, GLONASS, Galileo and BeiDou (see section 3.1).

2.3.2 Precise Orbit Determination Scenario

The goal of this observation scenario is to collect raw GNSS data using one antenna and one receiver. The observations are required for POD during post-processing. There are two different implementations. One uses only GPS data and one uses data from all four major GNSS constellations. The

Abbreviation	Explanation	Scenario
UBX-NAV-PVT	This message reports a position, velocity and time solution as well as various accuracy figures.	PVT, POD, attitude determination
UBX-NAV-POSECEF	This message provides a position solution in earth centred and earth fixed (ECEF) coordinates and the according accuracy estimate.	PVT, POD, attitude determination
UBX-NAV-VELECEF	This message provides a velocity solution in earth centred and earth fixed (ECEF) format and the according accuracy estimate.	PVT, POD, attitude determination
UBX-NAV-TIMEGPS	This message includes the precise GPS time of the most recent navigation solution as well as statements about its accuracy and validity.	PVT, POD, attitude determination
UBX-RXM-RAWX	This message provides raw GNSS measurements of all active GNSS including pseudorange, phase and Doppler measurements as well as signal quality information.	POD, attitude determination

Table 2: Abbreviation and explanation (u-blox AG, 2022a) of the enabled GNSS messages as well as the scenario they are used for

advantage of gathering only GPS data is that it requires less power and storing capacity. On the other hand, the redundancy is limited due to the lower number of observed satellites. This scenario runs on top of the nominal PVT mode and includes the additional message UBX-RXM-RAWX (see Table 2).

2.3.3 Attitude Determination Scenario

In order to compute a baseline in space and determine the attitude, this scenario collects raw GNSS data at a higher sampling rate using both antennas and receivers simultaneously. A high sampling rate, typically one second, allows detecting cycle slips in the phase observations. For this scenario, the four major GNSS constellations are considered. As well as the POD mode, it runs on top of the nominal PVT mode and requires the message UBX-RXM-RAWX (see Table 2) additionally.

2.4 Attitude Determination Experiment

To evaluate whether valid data is received while the satellite rotates for the generation of artificial micro- and milligravity, a test is set up. The following subsections describe the experiment in detail.

2.4.1 Study Design

Using a prototype of the satellite as well as a mount enabling the rotation of the prototype, the movement of the CubeSat while generating artificial gravity in space is imitated. Hence, the receipt of GNSS data can be experimentally tested under various configurations. On the one hand, static and kinematic GNSS data acquisition is performed to evaluate the impact of the rotation. On the other hand, the influence of the satellites coating on the noise behaviour is studied by conducting the experiment with and without solar panels attached to the satellite. Consequently, four different measurement epochs can be reported.

As the experiment is performed on Earth, it cannot exactly simulate the signal conditions in space. Nevertheless, it should give an overview whether valid data for the computation of a baseline can be gathered.

2.4.2 Hypotheses

Based on the different approaches to collect the data, the following null hypotheses can be set up:

1. While rotating, less satellites can be tracked.
2. The rotation has no influence on the noise behaviour.
3. The aluminium coating has a negative influence on the noise.

The goal of the experiment is to be able to reject the null hypotheses (Montello and Sutton, 2013).

2.4.3 Prototype

For the experiment, an empty envelope of the satellite as well as a mount enabling the rotation using an engine is built (see Figure 2). The envelope imitates the original CubeSat by using the same dimensions and the same material for the walls. These are made out of aluminium plates covered by solar panels. For the original CubeSat, on three longitudinal sides solar panels are attached but for the experiment only two sides can be covered due to material availability.

Likewise, the same antenna types, receiver types and other components as for the CubeSat are used (see section 2.1). In total, three antennas and receivers are mounted on the prototype to evaluate two possible baselines (consider Figure 1 for a sketch of the mounting spots and Figure 3 for the realised mounting spots). On the two longitudinal sides next to the side containing two of the GNSS antennas, the two solar panels are attached. It is assumed that the effect of the side opposite to the mounting spot of the antennas is negligible. The receivers are configured according to the attitude determination scenario (see section 2.3). To store the data, three data loggers, one for each receiver, are fixed to the inside of the envelope. A fourth logger is added to balance the weight and stabilize the rotation during the experiment.

2.4.4 Study Setup and Procedure

To perform the experiment, the test setup is mounted on a rooftop at ETH Honggerberg to enable receiving as much direct signal as possible (see Figure 2). As soon as the receivers record a fixed signal, the experiment starts by gathering data for ten minutes without rotation. This static measurements are used as a reference. After ten minutes, the motor is started to enable the rotation. Likewise, data is collected for ten minutes. During the two periods, the data is continuously recorded on the loggers in so-called ubx-files.

The experiment is conducted once without solar panels attached to the aluminium plate on May 4th 2023 and once with solar panels on May 9th 2023. The experiment is performed on two different days so that a similar satellite constellation can be expected. Therefore, the experiment with solar panels starts 20 minutes earlier to compensate for the shift between solar and sidereal time.

2.4.5 Data Analysis

The data recorded by the loggers are stored in ubx-files (see section 3.2). To analyse the data, the following steps are applied. First, the software *RTKLIB* is used to convert the ubx-files to the conventional RINEX-files and create various plots, including a sky-plot, plots of the signal-to-noise ratio (SNR) and a plot displaying the satellites' visibility (Tim Everett, 2021) (see section 4). To show the position of the satellites on a sky-plot, the broadcast ephemerides have to be added to the software (see section 3.3). Furthermore, information about the number of tracked satellites and the SNR of a certain frequency band can be exported. Specifically speaking, the software does not report the SNR although it labels it as such. In fact, the carrier noise density (C/N0) which is standardized per unit bandwidth is evaluated (Wahyudin Syam, 2023). To use the same designation as *RTKLIB*, this reports also refers to it as the SNR.

Second, two python scripts are coded to analyse the number of tracked satellites (*numSat_analysis.py*) and the SNR (*snr_analysis.py*) exported with *RTKLIB*. The script *numSat_analysis.py* allows

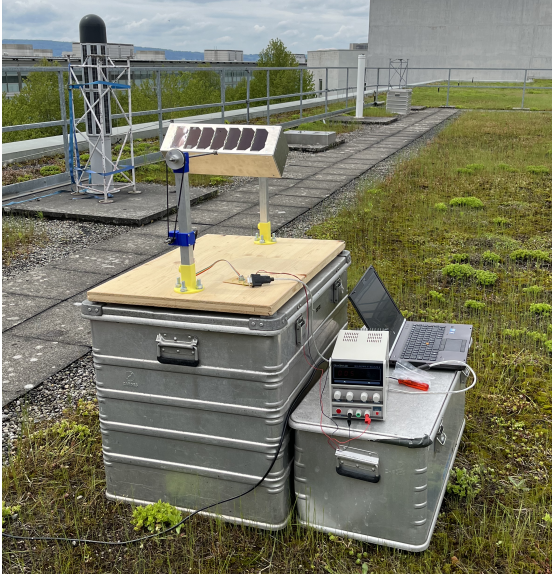


Figure 2: The experiment setup including the prototype, the mount and the engine

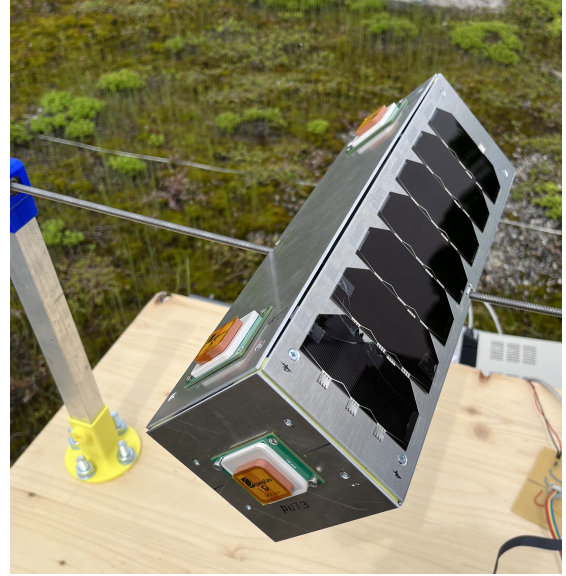


Figure 3: The prototype with solar panels and three antennas

to compute the mean of tracked satellites as well as to visualise the number of tracked satellites over time. Moreover, a bar chart can be created to compare the mean of tracked satellites under the four different conditions. The script can be used to test hypothesis 1. To validate the other hypotheses, the script *snr_analysis.py* is implemented calculating the standard deviation of the SNR to highlight its variation. It enables to compute the standard deviation of the SNR per satellite and measurement epoch as well as using error propagation to calculate the standard deviation of a whole measurement epoch (see Formula 1). The standard deviation is rounded to two decimal places as it is provided by *RTKLIB* with such accuracy. The analysis based on the measurement epochs is performed with an accuracy of one second. Due to the setup using a manually activated engine, it is not possible to time and evaluate the experiment more precisely. Both, the SNR and the standard deviation, can be plotted. The results are listed in section 4.

Moreover, the script *txt_ubx2csv.py* (see 2.2) can be used to parse the messages collected during the experiment. Therefore, the ubx-files recorded on the loggers are read and parsed.

$$\sigma_{overall} = \sqrt{\sigma_{sat_1}^2 + \sigma_{sat_2}^2 + \dots + \sigma_{sat_n}^2} \quad (1)$$

whereby

- n number of tracked satellites in one measurement epoch
- σ_{sat_n} standard deviation of the SNR of the n^{th} satellite, in dBHz
- $\sigma_{overall}$ standard deviation of the SNR over a measurement epoch, in dBHz

3 Data

The following subsections focus on GNSS data in general, the gathered data during the experiment as well as the broadcast ephemerides needed for the sky-plot.

3.1 GNSS data

As mentioned in section 2.1, the receivers in use are capable of tracking multiple GNSS constellations. For the SAGE mission, the US-American constellation GPS, the Russian constellation GLONASS, the European constellation GALILEO and the Chinese constellation BeiDou are used. Among others, these constellations differ in satellites, orbits and signal structure. Nevertheless, all the GNSS satellites send signals that enable real-time range measurements and data transmission. Hence, the GNSS observables are ranges measurements which can be determined by comparing the received signal and a receiver-generated replica. Either measured time or phase differences are used for such comparison. As the measurement principle follows the "one-way concept" from the satellite to the receiver, two clocks are involved to get the time difference, namely the satellite's and the receiver's clock. Therefore, the ranges are biased by the clock error and called pseudoranges. In general, the sent signals are composed of a carrier frequency in the L-band (e.g. L1 with 1575.42 MHz, L2 with 1227.60 MHz for GPS) which is modulated by a chip-sequence. The chip-sequence itself contains the data message modulated by the ranging code. (Hofmann-Wellenhof et al., 2008)

A small proportion of such data messages is listed in Table 2. The message names contain of the protocol name (e.g. UBX), the class name (e.g. NAV) and the message name (e.g. PVT), which are combined using hyphens. The messages itself are composed of several fields including the message identifier, the payload of variable length and the checksum. The latter is used to validate if a message is complete. The payload varies as it stores the information transmitted with a certain message. The information is clearly structured, containing elements and their values in a fixed order. While parsing the messages (see section 2.2), these elements and values can be extracted. (u-blox AG, 2022a)

3.2 Collected Data

For the experiment, the receivers are configured according to the attitude determination scenario to collect data (see section 2.1 for the configuration, section 2.3 for the scenario and section 2.4 for the experiment). Unfortunately, the configuration failed for ANT2 and ANT3 as both of them did not record the specified UBX-NAV-messages (see Table 2). This can be validated using the script *txt_ubx2csv.py* or the software *u-center*. Furthermore, ANT2 tracks with a higher sampling rate of 5 Hz instead of 1 Hz. To adjust the sampling rate, the software *RTKLIB* is used during post-processing.

The recorded ubx-files as well as the RINEX-files and exported txt-files from *RTKLIB* can be found in the supplementary material, in section "3_code" in the folder "data". Furthermore, there are some early testing files to show the functionality of the receivers and the coded scripts.

3.3 Broadcast Ephemerides

Broadcast ephemerides are one of three possible data sets to determine the position and velocity of satellites in a terrestrial reference frame. Based on observations at GNSS sites, they contain general information as well as information on the orbit and the satellite's clock. As they are part of the satellite message, they can be used to compute a reference orbit with meter-level accuracy (Hofmann-Wellenhof et al., 2008). The Crustal Dynamics Data Information System (CDDIS), NASA's archive of space geodesy data, provides daily broadcast ephemerides files which include all broadcast ephemerides messages required for post-processing (Noll, 2010). For this project, the "Daily RINEX V3 GPS Broadcast Ephemeris Files" of the respective days are used (Michael and Tyahla, 2023). These files are needed to enrich the observation data with navigation data so that a

3 Data

sky-plot of the tracked satellite can be generated (see section 2.4). As the other data, they can be found in the supplementary material, in section "3_code" in the folder "data".

4 Results

Using the script *numSat_analysis.py*, the number of tracked satellites for all antennas can be visualized (see Figure 4 and Figure 5, respectively without and with solar panels). During the second half of the experiment when the prototype rotates, the number of tracked satellites varies more. Considering the mean (see red dashed line in Figure 4 and Figure 5, for the exact values see Figure A.1 in the appendix), there is not much difference whether the prototype is covered with solar panels or not. To see the distribution of the tracked satellites, the sky-plots generated with *RTKLIB* (as a reference, see Figure A.2 in the appendix) can be considered.

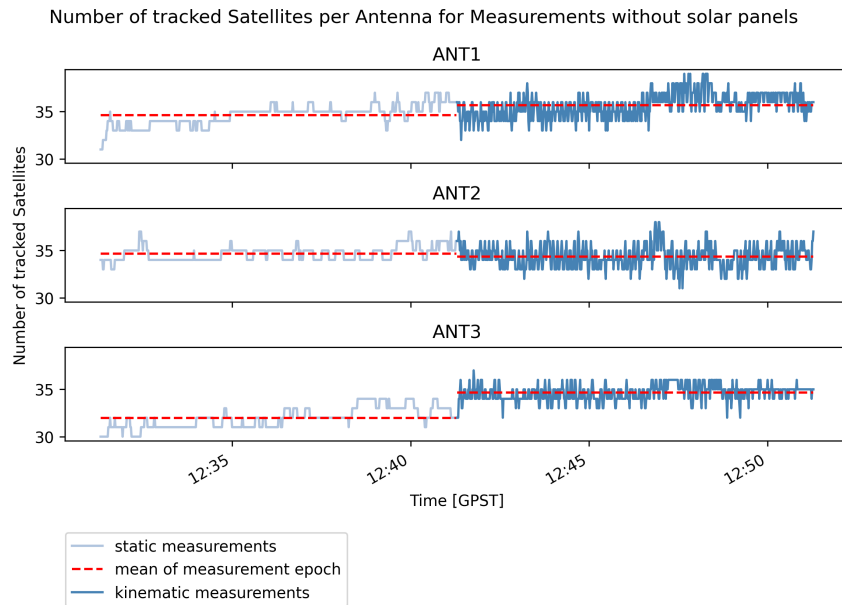


Figure 4: Number of tracked satellites during the experiment without solar panels

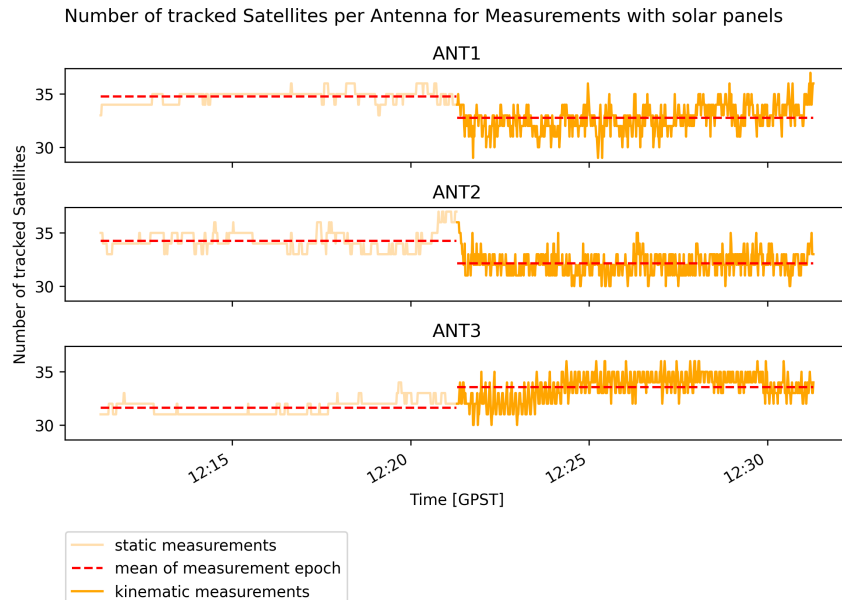


Figure 5: Number of tracked satellites during the experiment with solar panels

Analysing the SNR of the signals with L1 carrier wave results in Figure 6, visualising the overall standard deviations of the SNR. The variations within the SNR can also be seen if it is directly plotted for one satellite. In Figure 7 and Figure 8, the SNR of the satellite with the acronym G23, a GPS

4 Results

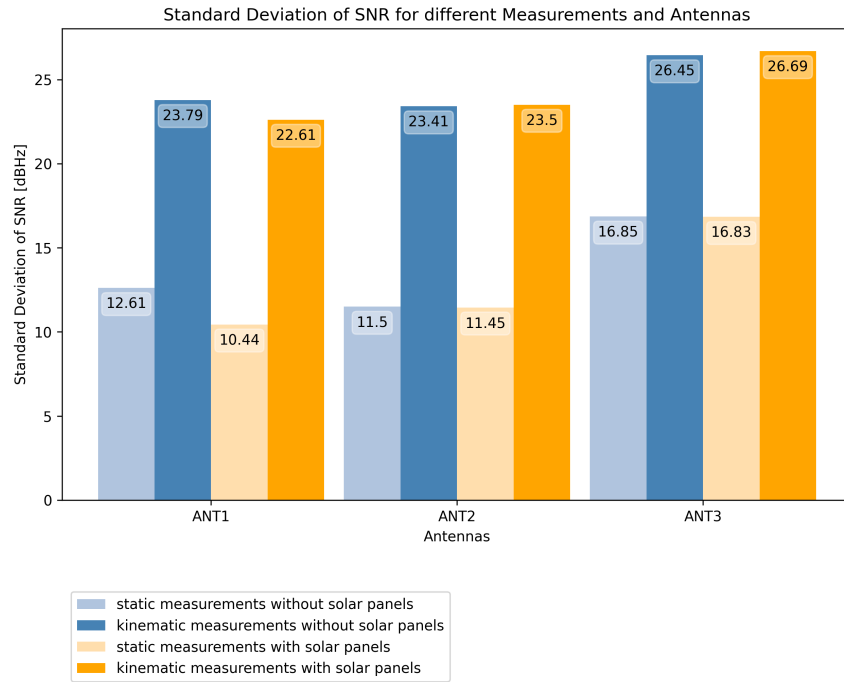


Figure 6: The standard deviation of the SNR for all antennas and measurement epochs computed using error propagation (see Formula 1)

satellite, is plotted. This satellite is chosen as it is regularly tracked with two frequencies during all measurement epochs.

The presented results as well as all the others generated can be found in the supplementary material, section "3_code" in the folder "output" and "plots". For each antenna and measurement epoch, the following results are available:

- csv-file storing the parsed UBX-NAV-messages
- csv-file storing the parsed raw data (UBX-RXM-RAWX-messages)
- csv-file storing the standard deviation and mean of the SNR of L1 and L2 per satellite
- plots generated using *RTKLIB*: sky-plots (e.g. Figure A.2), SNR-plots (e.g. Figure A.3), plots visualising the satellites' visibility (e.g. Figure A.4)

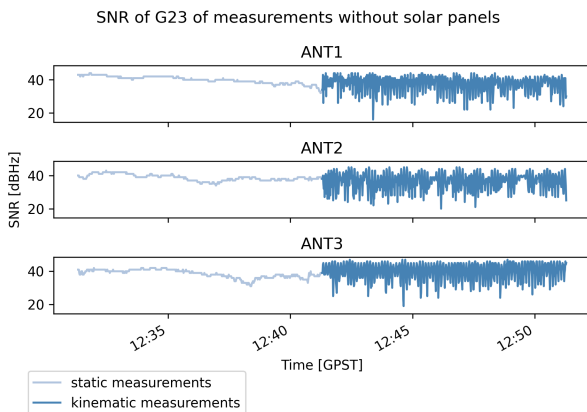


Figure 7: The SNR of the satellite G23 during the experiment without solar panels

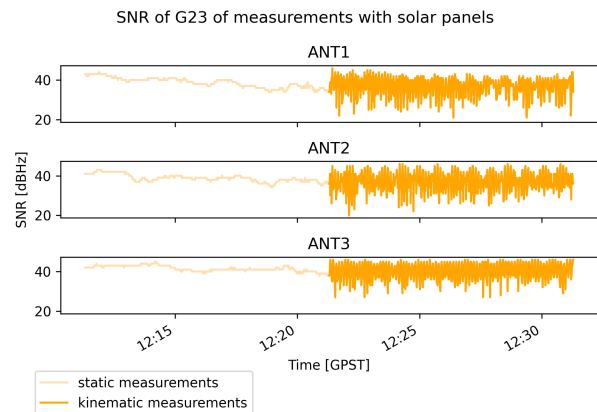


Figure 8: The SNR of the satellite G23 during the experiment with solar panels

- plots visualising the time series of the SNR for all satellites
- plots visualising the time series of the SNR for the satellites with the three highest and smallest standard deviations (e.g Figure A.5)

Moreover, there are results summarising information for all antennas:

- csv-file storing the overall standard deviation of the SNR of L1 and L2
- csv-file storing the mean of number of tracked satellites
- bar-charts visualising the data in the above mentioned csv-files (Figure 6, Figure A.1)
- plots visualising the time series of the number of tracked satellites (Figure 4, Figure 5)
- plots visualising the time series of the SNR for the satellite G23 (Figure 7, Figure 8)

Additionally, some early testing files for the scripts *txt_ubx2csv.py* and *ser_ubx2csv.py* are included to show their functionality.

5 Discussion

While analysing the results, it can be shown that during the rotation it is possible to track satellites continuously. Furthermore, satellites from more or less all elevation and azimuth angles can be detected during the experiment by all antennas (as a reference, see Figure A.2 in the appendix). Comparing the sky-plots and the variation of the SNR of different satellites (as a reference, see Figure A.5 in the appendix), there is hardly any relation between higher variations in SNR and location in the sky-plot. Nevertheless, satellites at lower elevations are more difficult to track continuously (as a reference, see Figure A.4).

Furthermore, the antennas mounted on the same side of the prototype, namely ANT1 and ANT2, show similar performance (see Figure 4, 5, 6, 7 and 8). ANT3 differs the most due to the slightly different geometry. Regarding the SNR, ANT3 generally shows more variation within the SNR (see Figure 6 and 7). This observation may occur due to the fact that the distance to the rotation axis is higher for ANT3 and the antenna partly faces the ground completely, or while in space, the Earth. In this particular position, it is not possible for the antenna to receive direct GNSS signals. Therefore, the SNR is typically lower. However, for all antennas the rotary movement can be detected as there is some periodicity within the SNR (see Figure 7 and 8). Moreover, during the rotation the variation is generally higher for the SNR and the number of tracked satellites (see Figure 4, 5 and 6). The explicit values of the standard deviation should be taken with caution as no outlier removal is performed. For future analysis, the outlier detection should be included. To have more redundancy, the experiment could as well be performed again. Additionally, it is crucial to check whether the receivers are correctly configured to avoid missing data (see section 3.2).

To assess the hypotheses (see section 2.4), the results presented in section 4 should be considered. Referring to Figures 4 and 5, hypothesis 1 cannot be fully rejected. With ANT3, it is possible to track more satellites during the rotation. Nevertheless, ANT1 and ANT2 tend to track slightly fewer satellites while rotating. This observation is enhanced for the experiment with solar panels. To analyse the influence of the solar panels in more depth, the SNR should be considered. However, for both conducts of the experiment, the variation in the number of tracked satellites is higher for the rotary phase. Whether this variation influences the computation of the baseline and thus the attitude determination badly, must be validated in a next step (see section 6). Furthermore, it should be checked if the higher number of tracked satellites is beneficial. If they can be tracked only for a very short period of time, it is assumed that there is no great benefit for the attitude determination.

Regarding hypothesis 2, the Figures 6, 7 and 8 clearly demonstrate that during the rotation the SNR varies more. The standard deviation of the SNR during the rotation is approximately twice the size of the standard deviation during the static measurements. Therefore, the rotation has a strong influence on the noise behaviour and the hypothesis can be rejected. Whether this effect is too high, considering the accuracy of the computed baseline, must be validated in the future (see section 6).

Comparing Figures 7 and 8, no great impact of the coating can be detected. Figure 6 supports this observation as per antenna the light blue bars are similar to the light orange one and the dark blue bars are similar to the dark orange ones. Thus, the standard deviation during static or kinematic measurements is comparable for the experiment with and without solar panels. The hypothesis 3 can be rejected. This result is not as intuitive as the one for hypothesis 2. For visual light, aluminium is more effected by reflection than solar panels due to the reflection coefficients of the materials. For solar panels, the reflection of incoming light is unfavourable as it equals loss of potential energy (Nell et al., 1991). However, as reflection and refraction is depending on the wave length (He et al., 1991), the properties of visual light cannot be compared to the ones of the GNSS signals. Nevertheless, multipath and refraction influence the noise. To assess the effect of the multipath, the methods suggested in Strode and Groves (2016) could be considered. During the mission of the CubeSat, this is not relevant as in space there will not be any multipath. In space, the influence of the refraction is more important. It is assumed that refraction can be beneficial and enables con-

tinuous satellite tracking as it allows to receive signals while the antennas partly face the ground or the Earth.

The above mentioned findings are based on the analysis of the SNR of L1. It is possible to evaluate the other carrier frequencies as well. The associated results of L2 are listed in the supplementary material (see 4). In general, they lead to comparable conclusions as for the frequency L1.

6 Conclusion and Outlook

For precise orbit and attitude determination, a GNSS payload board is foreseen on the SAGE CubeSat. Hence, this project focuses on defining the fundamental technical specifications, developing a parsing algorithm as a reference for the driver on the OBC and performing an experiment to validate various configurations. The CubeSat is equipped with two *ZED-F9P* receivers by u-blox and two low-cost antennas by Taoglas. Furthermore, splitters, low-noise amplifiers and filters are added. Depending on the observation scenarios, different GNSS data are received and parsed. The receiving of the signal is checked conducting an experiment with a prototype. It can be shown that during the rotation of the satellite, the number of tracked satellites as well as the SNR fluctuate more strongly. Nevertheless, the signals can be tracked continuously for some of the satellites.

To analyse the data of the experiment in more depth and to get more insight on the effect of the variations within the number of tracked satellites and SNR, the baseline between two different antennas should be computed. The calculated baseline should match the real baseline with mm- to cm-level accuracy. Due to the short length, the baseline is only affected by phase centre variation, geometric distance and receiver clock error as the data has been logged individually. The geometric distance can be extracted from Figure 1. Using the computed baseline, an algorithm to determine the attitude should be developed. It can be used to enrich the state estimation of the ADCS.

In the future, it could be considered to perform the experiment in a simulator that imitates the GNSS signal conditions in space (Deutsches Zentrum für Luft- und Raumfahrt, 2023). It is assumed that the data gathered in the simulator can be used to determine the attitude in more realistic conditions.

Moreover, the integration of GNSS payload board should be continued. Further specifications such as the runtime of the observation scenarios or the download rate should be defined in consultation with SAGE. The ADCS would like to foster the orbit propagation using the GNSS data.

Acknowledgement

I want to thank my supervisors, my team members at ARIS, especially Simon Tobler, Chantal Woodtli and Blanca Crazzolara, and Lukas Müller for their support during this project.

References

- ARIS (2023a). *SAGE CubeSat*. URL: <https://aris-space.ch/sage-cubesat/>.
- ARIS (2023b). *Space to Grow*. URL: <https://aris-space.ch>.
- Deutsches Zentrum für Luft- und Raumfahrt (2023). *MASTER (Multi-output Advanced Signal Test Environment for Receivers)*. URL: <https://www.dlr.de/de/forschung-und-transfer/forschungsinfrastruktur/grossforschungsanlagen/master>.
- He, X. D., Torrance, K. E., Sillion, F. X., and Greenberg, D. P. (1991). "A comprehensive physical model for light reflection." In: *ACM SIGGRAPH Computer Graphics* 25(4), pp. 175–186. doi: 10.1145/127719.122738.
- Hofmann-Wellenhof, B., Lichtenegger, H., and Wasle, E. (2008). *GNSS – Global Navigation Satellite Systems. GPS, GLONASS, Galileo & more*. Springer-Verlag.
- Infineon Technologies AG (2021). *BGB741L7ESD, Pre-matched general purpose LNA MMIC for 50 MHz-3.5 GHz applications (Data Sheet)*. Tech. rep. URL: https://www.infineon.com/dgdl/Infineon-BGB741L7ESD-DataSheet-v03_01-EN.pdf?fileId=5546d46265f064ff016638972c994ed7.
- Michael, P. and Tyahla, L. J. (2023). *CDDIS - Broadcast ephemeris data*. URL: https://cddis.nasa.gov/Data_and_Derived_Products/GNSS/broadcast_ephemeris_data.html.
- Mini-Circuits (n.d.[a]). *MMIC Surface Mount Power Splitter/Combiner GP2S1+ (Data Sheet)*. Tech. rep. URL: https://eu.mouser.com/datasheet/2/1030/GP2S1_2b-1700508.pdf.
- Mini-Circuits (n.d.[b]). *Ultra-Small Ceramic Power Splitter/Combiner QCN-19D+ (Data Sheet)*. Tech. rep. URL: https://eu.mouser.com/datasheet/2/1030/QCN_19D_2b-1701078.pdf.
- Montello, D. R. and Sutton, P. C. (2013). *An Introduction to Scientific Research Methods in Geography and Environmental Studies*. Ed. by R. Rojek, A. Clogan, K. Haw, and N. Dowden. second edition. SAGE Publications Ltd, pp. 200–202.
- Mouser Electronics Inc. (2023). *Mouser Electronics - RBBPF3225180C67B1U*. URL: https://www.mouser.ch/ProductDetail/Walsin/RBBPF3225180C67B1U?qs=ZrPdAQfJ6D0pS5Yxd810jQ%3D%3D&gclid=CjwKCAjwuqiiBhBtEiwATgvixIuM2f1Gb8tVEds7fDsTc0UWqWr8zeC9oiolzhG090_-TME5MwrYQRoC4SoQAuD_BwE.
- Nell, M. E. et al. (1991). "Design and Measurement of Antireflection Coatings for AlGaAs/GaAs Solar Cells." In: *Tenth E.C. Photovoltaic Solar Energy Conference*. Springer Netherlands, pp. 545–548. doi: 10.1007/978-94-011-3622-8{_}138.
- Noll, C. E. (2010). "The crustal dynamics data information system: A resource to support scientific analysis using space geodesy." In: *Advances in Space Research* 45(12), pp. 1421–1440. doi: 10.1016/j.asr.2010.01.018.
- Qorvo Inc. (2023). *Qorvo - TQP3M9036*. URL: <https://www.qorvo.com/products/p/TQP3M9036>.
- Strode, P. R. R. and Groves, P. D. (2016). "GNSS multipath detection using three-frequency signal-to-noise measurements." In: *GPS Solutions* 20(3), pp. 399–412. doi: 10.1007/s10291-015-0449-1.
- Taoglas (2021). *Datasheet GPSF.36.7.A.30*. Tech. rep. URL: <https://www.taoglas.com/datasheets/GPSF.36.7.A.30.pdf>.

- The European Space Agency (2020). *ENABLING & SUPPORT - Polar and Sun-synchronous orbit*. URL: https://www.esa.int/ESA_Multimedia/Images/2020/03/Polar_and_Sun-synchronous_orbit.
- Tim Everett (2021). *RTKLIB Code: Windows executables*. URL: <https://rtkexplorer.com/downloads/rtklib-code/>.
- Toorian, A., Diaz, K., and Lee, S. (2008). "The CubeSat Approach to Space Access." In: *2008 IEEE Aerospace Conference*. IEEE, pp. 1–14. DOI: 10.1109/AERO.2008.4526293.
- u-blox AG (2022a). *u-blox F9 HPG 1.32, u-blox F9 high precision GNSS receiver (Interface Description)*. Tech. rep. URL: https://content.u-blox.com/sites/default/files/documents/u-blox-F9-HPG-1.32_InterfaceDescription_UBX-22008968.pdf.
- u-blox AG (2022b). *u-center, GNSS evaluation software for Windows (User guide)*. Tech. rep. URL: https://content.u-blox.com/sites/default/files/u-center_Userguide_UBX-13005250.pdf.
- u-blox AG (2023). *ZED-F9P-04B, High precision GNSS module (Data sheet)*. Tech. rep. URL: https://content.u-blox.com/sites/default/files/ZED-F9P-04B_DataSheet_UBX-21044850.pdf.
- Wahyudin Syam (2023). *The difference between C/N0 and SNR in GNSS signal processing*. URL: <https://www.wasyresearch.com/the-difference-between-c-n0-and-snr-in-gnss-signal-processing/>.

Declaration of Originality



Eidgenössische Technische Hochschule Zürich
Swiss Federal Institute of Technology Zurich

Declaration of originality

The signed declaration of originality is a component of every semester paper, Bachelor's thesis, Master's thesis and any other degree paper undertaken during the course of studies, including the respective electronic versions.

Lecturers may also require a declaration of originality for other written papers compiled for their courses.

I hereby confirm that I am the sole author of the written work here enclosed and that I have compiled it in my own words. Parts excepted are corrections of form and content by the supervisor.

Title of work (in block letters):

A low-power GNSS payload board for precise orbit determination onboard the ARIS SAGE microgravity nanosatellite

Authored by (in block letters):

For papers written by groups the names of all authors are required.

Name(s):

Wicki

First name(s):

Juliette

With my signature I confirm that

- I have committed none of the forms of plagiarism described in the '[Citation etiquette](#)' information sheet.
- I have documented all methods, data and processes truthfully.
- I have not manipulated any data.
- I have mentioned all persons who were significant facilitators of the work.

I am aware that the work may be screened electronically for plagiarism.

Place, date

Zurich, 15 June 2023

Signature(s)

For papers written by groups the names of all authors are required. Their signatures collectively guarantee the entire content of the written paper.

A Some Additional Results

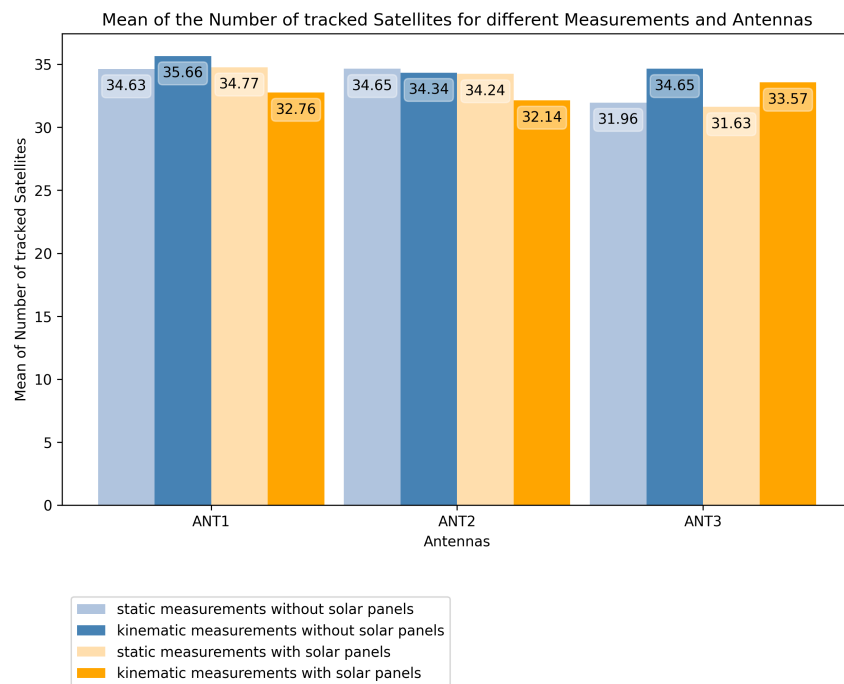


Figure A.1: For each antenna and measurement epoch the mean of the number of tracked satellites is displayed

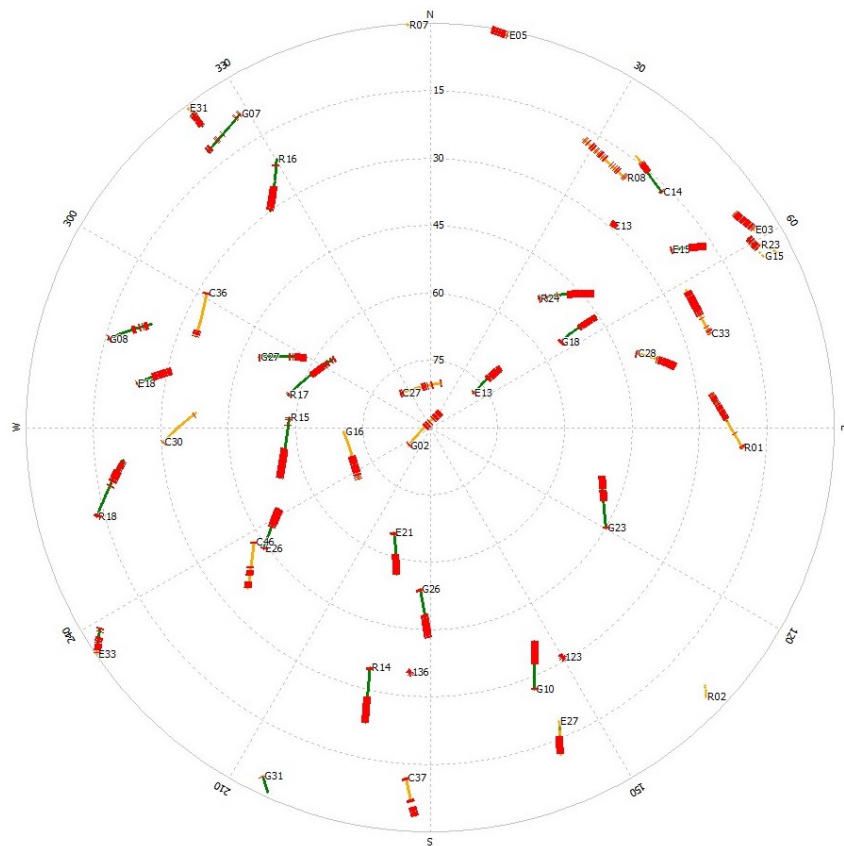


Figure A.2: Sky-plot of ANT1 during the experiment without solar panels, generated using *RTKLIB*

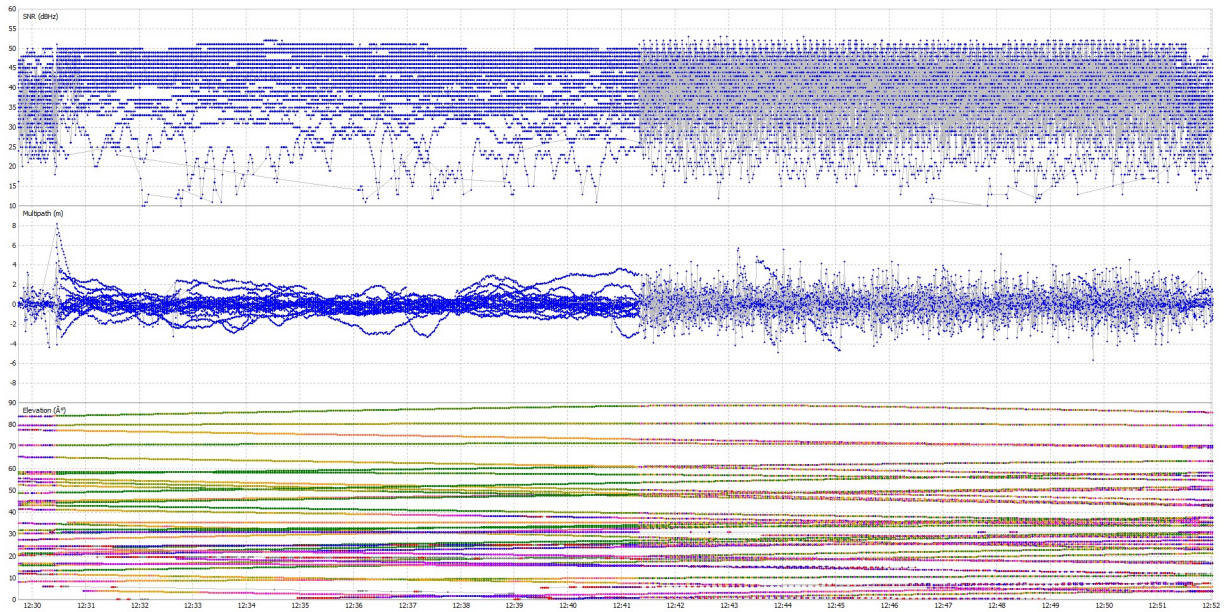


Figure A.3: SNR of L1, multipath and elevation of satellites tracked by ANT1 during the experiment without solar panels, generated using *RTKLIB*

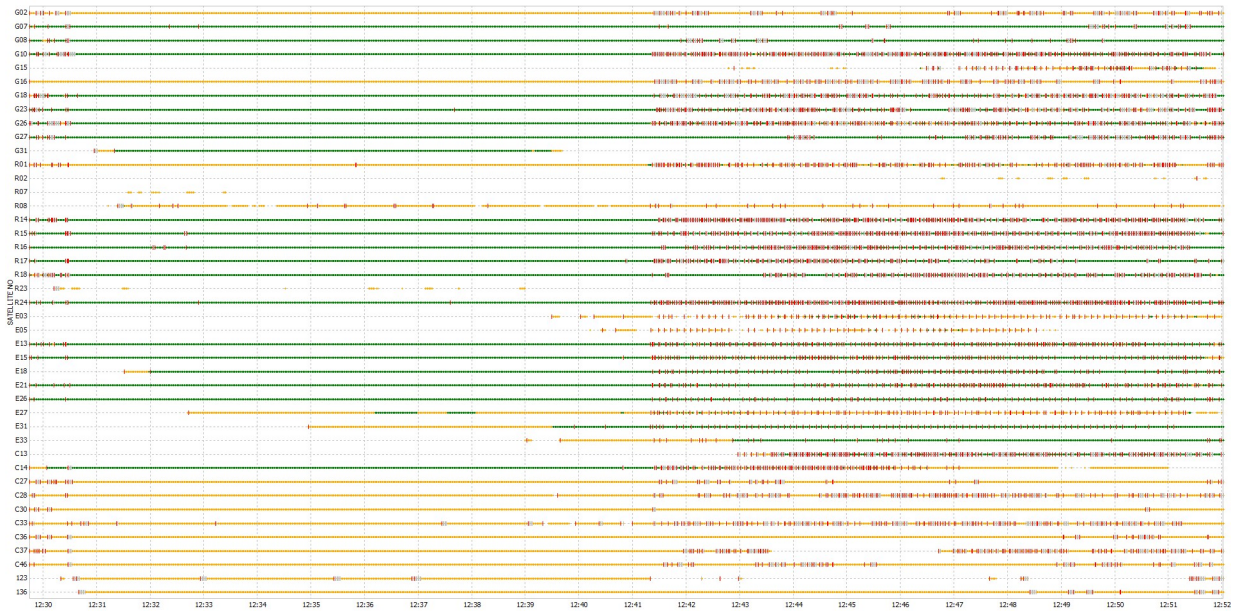


Figure A.4: Satellites tracked by ANT1 during the experiment without solar panels, generated using *RTKLIB*, color-coding represents number of tracked frequencies (green: 2 frequencies, yellow: 1 frequency)

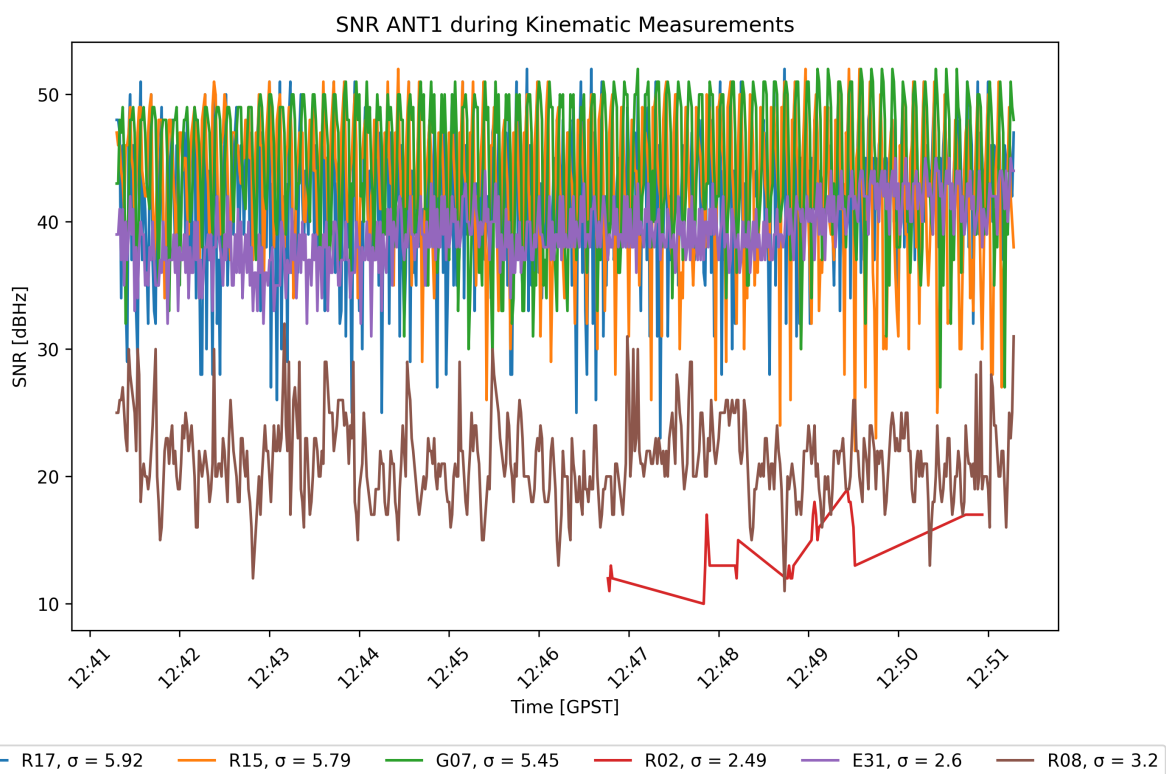


Figure A.5: SNR of L1 of the satellites tracked by ANT1 with the three highest and smallest standard deviations during the experiment without solar panels